

Sub-Poissonian shot noise of a high internal gain injection photon detector

Omer Gokalp Memis,¹ Alex Katsnelson,¹ Soon-Cheol Kong,¹ Hooman Mohseni,^{1,*} Minjun Yan,² Shuang Zhang,² Tim Hossain,² Niu Jin,² and Ilesanmi Adesida²

¹ Bio-Inspired Sensors and Optoelectronics Laboratory, Dept. of Electrical Engineering and Computer Science, Northwestern University, Evanston, IL 60208

² Micro and Nanotechnology Laboratory, University of Illinois at Urbana-Champaign, IL 61801

*Corresponding author: hmohseni@eecs.northwestern.edu

Abstract: The noise performance of an infrared injection photon detector with very high internal gain was investigated at a wavelength of 1.55 μm . The devices showed sub-Poissonian shot noise with Fano factors around 0.55 at 0.7 V at room temperature. Optical to electrical conversion factors of 3000 electrons per absorbed photon were recorded at 0.7 V. The change in noise-equivalent power with respect to bias voltage was evaluated. The optical to electrical conversion factor and Fano factor were measured under increasing illumination and compared to theoretical expectations.

©2008 Optical Society of America

OCIS codes: (040.5160) Photodetectors; (040.3060) Infrared; (040.3780) Low light level.

References and links

1. P. J. Edwards, "Sub-Poissonian electronic and photonic noise generation in semiconductor junctions," *Aust. J. Phys.* **53**, 179-192 (2000).
2. G. Kiesslich, H. Sprekeler, A. Wacker, and E. Scholl, "Positive correlations in tunnelling through coupled quantum dots," *Semicond. Sci. Technol.* **19**, S37-S39 (2004).
3. I. A. Maione, M. Macucci, G. Iannaccone, G. Basso, B. Pellegrini, M. Lazzarino, L. Sorba, and F. Beltram, "Probing Pauli blocking with shot noise in resonant tunneling diodes: Experiment and theory," *Phys. Rev. B* **75**, 125327 (2007).
4. V. Y. Aleshkin, L. Reggiani, N. V. Alkeev, V. E. Lyubchenko, C. N. Ironside, J. M. L. Figueiredo, and C. R. Stanley, "Giant suppression of shot noise in double barrier resonant diode: a signature of coherent transport," *Semicond. Sci. Technol.* **18**, L35-L38 (2003).
5. A. Wacker, E. Schöll, A. Nauen, F. Hohls, R. J. Haug, G. Kiesslich, "Shot noise in tunneling through a quantum dot array," *Phys. Status Solidi C* **0**, 1293-1296 (2003).
6. G. Ribordy, N. Gisin, O. Guinnard, D. Stucki, M. Wegmuller, and H. Zbinden, "Photon counting at telecom wavelengths with commercial InGaAs/InP avalanche photodiodes: current performance," *J. Mod. Optic.* **51**, 1381-1398 (2004).
7. R. J. McIntyre, "Multiplication Noise in Uniform Avalanche Diodes," *IEEE Tran. Electron Dev.* **13**, 164-168 (1966).
8. F. Z. Xie, D. Kuhl, E. H. Botcher, S. Y. Ren, and D. Bimberg, "Wide-Band Frequency-Response Measurements of Photodetectors Using Low-Level Photocurrent Noise Detection," *J. Appl. Phys.* **73**, 8641-8646 (1993).
9. Y. L. Goh, J. S. Ng, C. H. Tan, W. K. Ng, and J. P. R. David, "Excess noise measurement in $\text{In}_{0.53}\text{Ga}_{0.47}\text{As}$," *IEEE Photonic Tech. L.* **17**, 2412-2414 (2005).
10. K. S. Lau, C. H. Tan, B. K. Ng, K. F. Li, R. C. Tozer, J. P. R. David, and G. J. Rees, "Excess noise measurement in avalanche photodiodes using a transimpedance amplifier front-end," *Meas. Sci. Technol.* **17**, 1941-1946 (2006).
11. O. G. Memis, S. C. Kong, A. Katsnelson, H. Mohseni, M. Yan, S. Zhang, N. Jin, and I. Adesida, "A photon detector with very high gain at low bias and at room temperature," *App. Phys. Lett.* **91**, 171112 (2007)
12. O. G. Memis, A. Katsnelson, H. Mohseni, M. Yan, S. Zhang, N. Jin, and I. Adesida, "On the Source of Jitter in a Room Temperature Nano-Injection Photon Detector at 1.55 μm ," *IEEE Electron Device Lett.* (to be published)
13. S. Cova, M. Ghioni, A. Lotito, I. Rech, and F. Zappa, "Evolution and prospects for single-photon avalanche diodes and quenching circuits," *J. Mod. Optic.* **51**, 1267-1288 (2004).
14. F. Z. Xie, D. Kuhl, E. H. Botcher, S. Y. Ren, and D. Bimberg, "Wide-band frequency response measurements of photodetectors using low-level photocurrent noise detection," *J. Appl. Phys.* **73**, 8641 (1993).

1. Introduction

Sensitivity of a photodetector is considered an important benchmark for most applications and therefore decreasing the noise levels is very attractive. The noise performance of most photon detectors targeting extremely low light levels, such as single photon detectors (SPDs), is limited by the current shot noise. In practice, the detector signal should not only surpass the detector noise, but also the electronic noise of the readout circuits and hence, having a high internal gain in addition to a low noise level is highly desirable. Here, we report on the sub-Poissonian shot noise performance of a new photon detector with previously reported internal gain values as high as several thousands.

Going beyond the classical limit for shot noise, devices with sub-Poissonian (suppressed) shot noise have been demonstrated. This phenomenon, called Fano effect [1], is shown to result from temporal correlation mechanisms influencing particle flow, such as Coulomb blockade [2] or Pauli exclusion principle [3]. The Fano factor has been shown to assume values as low as 0.4 by imposing temporal correlations of charged carriers [4]. The strength of shot noise suppression (or enhancement) is quantified by the Fano factor [5] γ as

$$\gamma = \frac{I_n^2}{I_{shot}^2} = \frac{I_n^2}{2qI_{DC}\Delta f} \quad (1)$$

where I_n is the measured standard deviation of current, or current noise; I_{shot} is the Poissonian shot noise; q is electron charge; I_{DC} is the average value of current; and Δf is the bandwidth. Note that Fano devices generally do not have an associated gain, and thus the right hand side of this equation is only valid for such devices. For devices with internal amplification, the denominator of the right hand side needs to be modified into $2qM^2I_{DC}\Delta f$. This is because of the amplification that applies to both the signal and the noise, and hence the noise power needs to be scaled by M^2 to conserve signal-to-noise (SNR)

Among the approaches used for single photon detection with internal gain, InGaAs/InP avalanche photodetectors (APDs) with avalanche gain mechanism offer high sensitivities for near-infrared (NIR) spectra beyond $\lambda \sim 1 \mu\text{m}$ [6]. However, avalanche gain has been shown to possess a statistical variance due to the unpredictable nature of collisions and ionizations involved [7]. The bidirectional multiplication mechanism and its unpredictable time-evolution make the effective multiplication values different for each carrier, increasing uncertainty and resulting in elevated noise levels and Fano factor. Traditionally, the excess noise factor F is used instead of the Fano factor γ as the merit of noise performance in APDs. Similar to Fano factor, excess noise factor is defined [8] as the measured deviation from the predicted multiplied by shot noise as

$$F = \frac{I_n^2}{2qM^2I_{int}\Delta f} \quad (2)$$

where I_n is the standard deviation of current, or current noise; q is electron charge; M is the multiplication factor or gain; I_{int} is the average value of current before it undergoes multiplication; and Δf is the bandwidth. Measurements on InGaAs/InP based APDs show a very rapid increase in excess noise factor with increasing gain. For instance, excess noise factors greater than 5 were measured [9,10], at multiplication values around 15.

2. Device structure and operating principle

To overcome noise limitations of available SPDs for the NIR range, we developed an avalanche-free infrared detector [11]. It is based on InP/GaAsSb/InGaAs material system and therefore has type-II band alignment, with the GaAsSb layer acting as a barrier for electrons

and a trap for holes. As detailed in [11], the active device structure consists of 1000 nm $\text{In}_{0.53}\text{Ga}_{0.47}\text{As}$ (n-doped, 10^{15} cm^{-3}), 50 nm $\text{GaAs}_{0.51}\text{Sb}_{0.49}$ (p-doped, $5 \times 10^{18} \text{ cm}^{-3}$) and 500 nm InP (n-doped, 10^{17} cm^{-3}), from bottom to up. The diameter of the InP injector is in the range of 100 nm to 15 μm for different devices. When the device is biased, the conduction band barrier due to the band lineup limits the flow (injection) of electrons, and the height of this barrier is controlled by the hole flux originating from the photo-absorption. With an optical excitation, optically generated holes increase the total hole flux, which then lowers the GaAsSb barrier where they are trapped. As a result, the lowered barrier allows more electron injection, and the number of injected electrons increases exponentially based on Fermi statistics. One possible explanation for the measured low-noise behavior of the device is the negative potential feedback mechanism in the device. Even though the voltage of the barrier is mainly controlled by hole flux, the injected electrons also play an important role in the regulation of barrier layer voltage. Compared to holes, which are trapped in the GaAsSb barrier for a relatively long time, electrons have a very short but finite transit time through the barrier. During the transit time they lower the local potential and increase the barrier height. The increase in barrier height opposes the flow of electrons and reduces the transmission probability. In a different study [12], we have shown that the jitter in passivated, very high speed injection detectors is 15 ps, and this value is almost entirely due to the variations in carrier transport delay, leaving a negligible contribution from the amplification mechanism and associated negative feedback. Hence, we believe that this negative feedback is fast enough to prevent temporal and spatial bunching of carriers, regulating the flow due to drift and diffusion. We believe that as a result of this regulatory negative feedback, the variance on gain is reduced below Poissonian shot noise expectation even at gain values as high as several thousands. In contrast to avalanche multiplication, which provides a positive-feedback [13] leading to associated instability, injection-based amplification mechanism promotes stability.

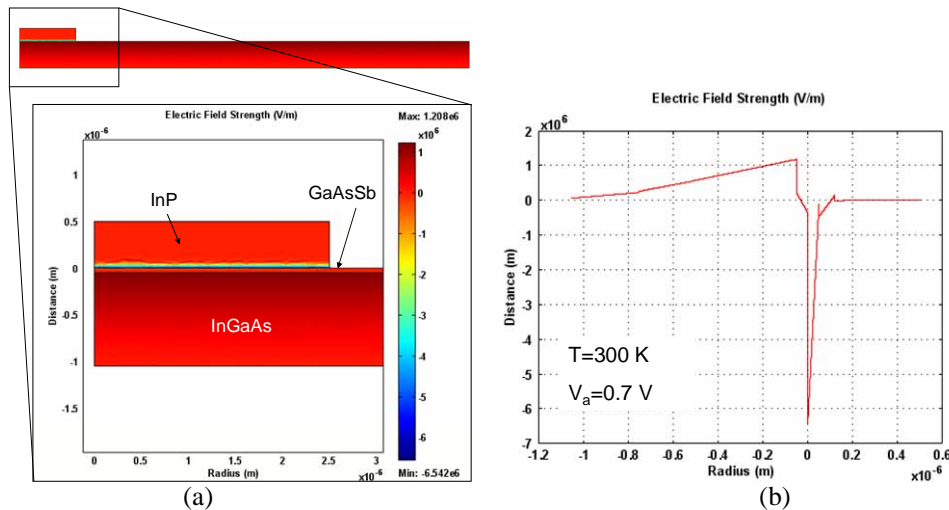


Fig. 1. (a). The device cross section, showing the electric field distribution at room temperature at 0.7 V bias. The bottom image shows zooms in the central region and labels the different layers of the device. (b). The electric field strength (V/m) along the central axis ($r=0$) of the device at 0.7 V at room temperature.

3. Experimental results

We measured the dark current, photo-response and spectral noise power of the devices at room temperature. At each data step the dark current and spectral noise power measurements were taken simultaneously, quickly followed by photocurrent measurements. During photocurrent measurements, the devices were illuminated with a CW laser at 1550 nm, which

was focused into a spot of approximately 5 μm in diameter, located 5 μm away from the injector of the device under test. The signal was amplified using a trans-impedance amplifier and recorded by a high accuracy multimeter and a spectrum analyzer. For laser power calibration, a commercial PIN detector was placed inside the setup as a separate experiment and its response was measured to accurately quantify the laser power reaching the sample.

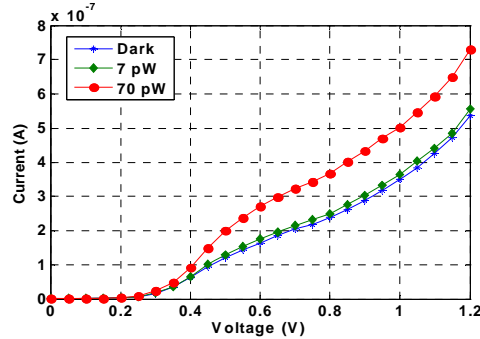


Fig. 2. The current-voltage plots at different optical illumination levels. (star) dark-current, (diamond) current at 7 pW, (circle) current at 70 pW.

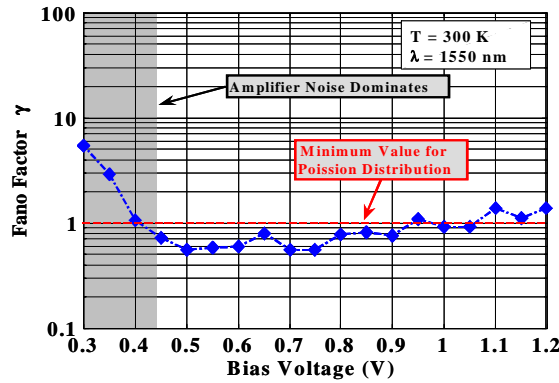


Fig. 3. Fano factor versus bias voltage. The device shows Fano factors less than 1, which indicates that the shot noise of the device has lower variance than Poissonian shot noise. At low voltages, the measured noise and corresponding Fano factor get affected by the noise floor of the setup.

Since detection and amplification mechanisms are tightly coupled in our detector, we had to identify the components of responsivity. Responsivity R is

$$R = \frac{q}{E_{ph}}(1-r)(1-e^{-\alpha L})\eta_c M \quad (3)$$

where q is electron charge, E_{ph} is photon energy (~ 0.8 eV here), r is reflection from the air-semiconductor boundary ($\sim 30\%$), α is InGaAs absorption coefficient ($\sim 1 \mu\text{m}^{-1}$ at $\lambda=1.55 \mu\text{m}$), L is the path length in InGaAs absorption layer ($1 \mu\text{m}$), η_c is carrier collection efficiency and M is the internal electrical gain. Among these factors, collection efficiency and gain are the unknowns and they could not be separately identified in the measurements. In our experiments, we have measured the responsivity using the dark and photocurrent measurements with a calibrated laser source. Then using the relation above, we have calculated the product $\eta_c M$, and adopted the product of gain and collection efficiency as the “effective optical-electrical conversion factor” ($\eta_c M$). In other words, optical-to-electrical conversion factor corresponds to the number of the electrons flowing through the device per an absorbed photon. Our simulation model predicts that the collection efficiency for our

device is around 70%. However, we have not incorporated this number into further calculations, as it is not a physical or measured value. Instead, we took the conservative approach of equating the gain to the optical-to-electrical conversion efficiency: The conversion factor is always smaller than the internal gain, since the collection efficiency is always less than unity.

Similar to [14], the spectral noise power after amplification was measured with a spectrum analyzer around 1.5 kHz, which is beyond the 1/f noise knee but lower than the measured bandwidth of the device of about 4 kHz. The measured spectral power was compared to predicted spectral noise density due to Poissonian shot noise with amplification ($2qM^2I_{in}\Delta f$) and Fano factor was calculated.

Devices with 10 μm injectors were tested. As previously reported [11], the spatial scans on the devices showed an active area that extended to 7-8 μm away from the injector, resulting in a total active diameter of $\sim 25 \mu\text{m}$. The devices showed high stable optical-electrical conversion factors around 3000 at 0.7 V and 5000 at around 1 V, indicating an internal gain that can extend beyond 5000. The measured Fano factor was $F \sim 0.55$ at such high gain values (see Fig. 3). Since we do not know the exact value of the internal gain, we took a conservative approach and used the optical-electrical conversion factor as if $\eta_c = 1$. This would always lead to an overestimation of the Fano factor. For instance, assuming a collection efficiency of 70% yields a Fano factor $F \sim 0.39$, which would mean the Poissonian shot noise is further suppressed in reality. However, using optical-electrical conversion factor as gain becomes a poor assumption at high optical intensities. As the incident optical power was increased, the measurements showed an overall decrease in optical-electrical conversion factor (Fig. 4), which is a result of decreasing collection efficiencies. Low collection efficiency is mainly due to carrier shielding and device saturation at high optical intensities. As the holes are collected from the large absorption region and drawn into the small GaAsSb volume, the hole current density shows a rapid increase in the radial direction towards the center. The high density of holes at the center of the device repels the incoming hole flux through Coulomb forces and introduces carrier shielding. The collection efficiency η_c drops more as the carrier shielding becomes more pronounced at stronger illumination. The effect of lowered collection efficiency manifests itself as low optical-electrical conversion factors and an overall increase in Fano factor at high intensities.

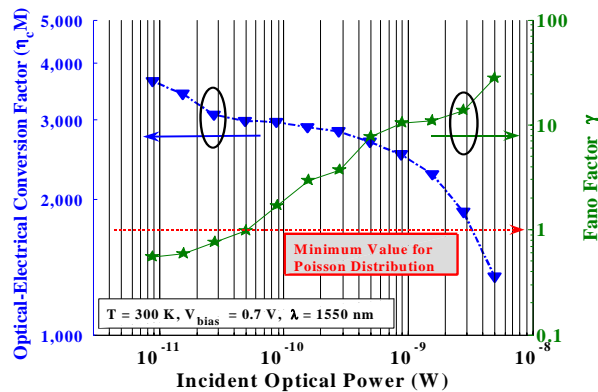


Fig. 4. Optical-electrical conversion factor and Fano factor versus optical intensity, measured at 0.7 V at room temperature. Due to carrier shielding and device saturation, optical to electrical conversion factors decrease at high optical intensities. Since the gain is assumed to be the equal to optical to electrical conversion factor in the calculation of Fano factor, the gain is underestimated and Fano factor is overestimated.

The noise equivalent power (NEP) of the devices was measured as $4.5 \text{ fW/Hz}^{0.5}$ at room temperature without any gating, using the relation

$$P_{NEP} = \frac{I_{n,meas}}{\eta_c M}, \quad (4)$$

which equates $I_{n,meas}$ (the measured spectral current noise in $A/Hz^{0.5}$) to the photocurrent that gives a unity signal to noise ratio. The change in NEP versus bias voltage is plotted in Fig. 5. Here we see that the optimum bias voltage for this detector is around 0.6-0.7 V, which is in agreement with the expectations from the band lineup and built-in potentials. Below 0.5 V, the electron injection through the InP-GaAsSb junction is the bottleneck of the transport across the device. When biased slightly above this critical point (0.5 V), the transport through this junction starts to increase rapidly. This bias point is where the device exhibits a low electron injection (i.e. low dark current, and low noise) with high sensitivity, which makes this bias more favorable than higher voltages. Hence the lowest NEP is achieved around these bias voltages. Comparing these values with a survey for detectors operating at 1.55 μm wavelength [15], we see that uncooled avalanche photo detectors can provide similar NEP values around a few $fW/Hz^{0.5}$ (1-2.2 $fW/Hz^{0.5}$). PIN detectors, which do not provide internal amplification, can achieve NEP on the order of $aW/Hz^{0.5}$ with cooling.

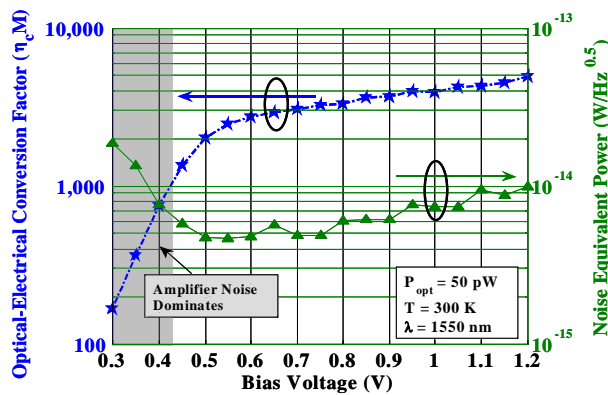


Fig. 5. Noise equivalent power and optical conversion factor versus bias voltage. The device shows optical to electrical conversion factors reaching 5000 at bias voltages less than 1.2 V. Noise equivalent power of the device is $4.5 fW/Hz^{0.5}$ at the optimal bias voltage ~ 0.7 V.

4. Conclusion

In conclusion, we report the sub-Poissonian shot noise performance of a new detector with internal gain values as high as 5000. Fano factors around 0.55 have been experimentally measured at room temperature. We attribute the low Fano factors to the internal feedback mechanism stabilizing the gain. Device behavior at high optical intensities was evaluated and the mechanism of device saturation due to carrier shielding was discussed, including its effect on gain and Fano factor. We believe that the high gain and low noise properties are very attractive for many low light applications and in particular, they would be useful ultra-low light infrared imagers where noise contamination from electronic noise of proceeding readout circuitry is the limiting performance.

Acknowledgments

This work is partly supported by National Science Foundation award # ECCS-0547227/A001 (to H.M.), and Defense Advanced Research Projects Agency award # HR0011-05-1-0058/P00006 (to H.M and I.A.).